

# Electronic excitations in $\text{ZnWO}_4$ and $\text{Zn}_x\text{Ni}_{1-x}\text{WO}_4$ ( $x = 0.1 - 0.9$ ) using VUV synchrotron radiation

Research Article

Aleksandr Kalinko<sup>1\*</sup>, Alexey Kotlov<sup>2</sup>, Alexei Kuzmin<sup>1†</sup>, Vladimir Pankratov<sup>1</sup>, Anatoli I. Popov<sup>1,3</sup>, Liana Shirmane<sup>1</sup>

<sup>1</sup> Institute of Solid State Physics, University of Latvia,  
Kengaraga street 8, LV-1063, Riga, Latvia

<sup>2</sup> Hamburger Synchrotronstrahlungslabor HASYLAB at Deutsches Elektronensynchrotron DESY,  
Notkestraße 85, Hamburg 22607, Germany

<sup>3</sup> Institute Laue Langevin,  
6 rue Jule Horowitz, 38042, Grenoble, France

Received 21 June 2010; accepted 13 October 2010

## Abstract:

The photoluminescence spectra and luminescence excitation spectra of pure microcrystalline and nano-sized  $\text{ZnWO}_4$  as well as the  $\text{Zn}_x\text{Ni}_{1-x}\text{WO}_4$  solid solutions were studied using vacuum ultraviolet (VUV) synchrotron radiation. The samples were also characterized by x-ray powder diffraction. We found that: (i) the shape of the photoluminescence band at 2.5 eV, being due to radiative electron transitions within the  $[\text{WO}_6]^{6-}$  anions, becomes modulated by the optical absorption of  $\text{Ni}^{2+}$  ions in the  $\text{Zn}_x\text{Ni}_{1-x}\text{WO}_4$  solid solutions; and (ii) no significant change in the excitation spectra of  $\text{Zn}_{0.9}\text{Ni}_{0.1}\text{WO}_4$  is observed compared to pure  $\text{ZnWO}_4$ . At the same time, a shift of the excitonic bands to smaller energies and a set of peaks, attributed to the one-electron transitions from the top of the valence band to quasi-localized states, were observed in the excitation spectrum of nano-sized  $\text{ZnWO}_4$ .

**PACS (2008):** 78.55.Hx, 81.07.Wx, 71.35.-y

**Keywords:**  $\text{ZnWO}_4$  •  $\text{Zn}_x\text{Ni}_{1-x}\text{WO}_4$  solid solutions • tungstates • electronic excitations • luminescence • VUV spectroscopy

© Versita Sp. z o.o.

## 1. Introduction

Sanmartinite ( $\text{ZnWO}_4$ ) belongs to a wide group of wolframite-type tungstates having the general formula  $\text{AWO}_4$  with  $\text{A}^{2+} = \text{Mg}^{2+}, \text{Mn}^{2+}, \text{Fe}^{2+}, \text{Co}^{2+}, \text{Ni}^{2+}, \text{Zn}^{2+}$ ,

and  $\text{Cd}^{2+}$  [1]. It is a technologically important material, which finds applications such as scintillation detectors, laser-active hosts, optical fibers, sensors, and phase-change optical recording media [2–7]. In addition,  $\text{ZnWO}_4$  shows highly efficient (> 50%) picosecond multiple Stokes and anti-Stokes generation when used as a Raman-active crystal in solid-state lasers, based on stimulated Raman scattering (SRS) [5, 8]. In the latter case, the strong SRS-active Raman mode at  $907 \text{ cm}^{-1}$  is

\*E-mail: akalin@latnet.lv (Corresponding author)

†E-mail: a.kuzmin@cfi.lu.lv

the internal stretching W–O  $A_g$ -mode in the  $WO_6$  octahedra [5, 8]. The tuning of the mode frequency can be achieved in tungstate solid solutions. Three such systems are known based on zinc tungstate:  $ZnWO_4$ – $FeWO_4$  [9],  $ZnWO_4$ – $MnWO_4$  [9], and  $ZnWO_4$ – $NiWO_4$  [10]. The latter system finds also application as a yellow ceramic pigment [10].

The optical and luminescent properties of wolframite-type  $ZnWO_4$  have been widely studied in the past more than once. In particular, the intrinsic luminescence band, observed at room temperature at about 2.5 eV, has been attributed to a charge transfer between oxygen and tungsten ions in the  $[WO_6]^{6-}$  anions [11–14]. The contributions from defects and distorted tungsten–oxygen octahedra have been also observed [15–17]. Up to now, most fundamental studies on tungstates have been performed on single-crystal samples. In this work we present the results on nano-sized  $ZnWO_4$  and microcrystalline  $Zn_xNi_{1-x}WO_4$  solid solutions using vacuum ultraviolet (VUV) synchrotron radiation spectroscopy.

## 2. Experiment

Pure  $ZnWO_4$  and the solid solutions  $Zn_xNi_{1-x}WO_4$  ( $x = 0.1 - 0.9$ ) were synthesized using a co-precipitation technique [18, 19]. All chemicals used were analytic grade reagents (purity 99%, “Reahim”) without further purification. Pure  $ZnWO_4$  was prepared by the reaction of  $ZnSO_4 \cdot 7H_2O$  and  $Na_2WO_4 \cdot 2H_2O$  at room temperature (20°C), pH 8, and a reaction time of 1–2 hours. The water solutions of the two salts were prepared by dissolving 10 mmol of the salt in 100 ml of double-distilled water with vigorous stirring. Next they were mixed in 1:1 molar ratio, and white precipitates appeared immediately. After completion of the precipitate reaction, the precipitate was filtered off, washed several times with distilled water, and dried in air for 12 hours at 80°C thus resulting in the white-colored nano-sized  $ZnWO_4$  powder [19]. Previous structural studies indicated that the  $ZnWO_4$  powder as prepared has particles of size below 2 nm and a relaxed  $ZnWO_4$  structure [19]<sup>1</sup>.

The nano-sized powder was next annealed in air for 4 hours at 400°C and 800°C. Annealing above 400°C results in the growth of crystallites, so that material becomes microcrystalline [19]. The yellow-colored solid solutions  $Zn_xNi_{1-x}WO_4$  ( $x = 0.1 - 0.9$ ) were prepared by first

mixing proper amounts of water solutions of  $ZnSO_4 \cdot 7H_2O$  and  $Ni(NO_3)_2 \cdot 6H_2O$  salts and further following the same preparation procedure. After drying, the obtained solid solutions were annealed in air for 4 hours at 800°C. The samples’ crystallinity and phase composition (formation of solid solution) were controlled by x-ray powder diffraction (XRD). The XRD patterns (Fig. 1) were recorded at 20°C using a Bragg–Brentano powder diffractometer with a graphite monochromator in the diffracted beam to eliminate the specimen’s fluorescence. A conventional tube with a copper anode (Cu  $K\alpha$  radiation) was used as x-ray source. The measurements were performed in the angle range  $2\theta = 5 - 70^\circ$  with the step  $\Delta(2\theta) = 0.05^\circ$ . The XRD data (ICSD No. 81937) for monoclinic ( $P2/c$ )  $ZnWO_4$  from [20] were used for comparison.

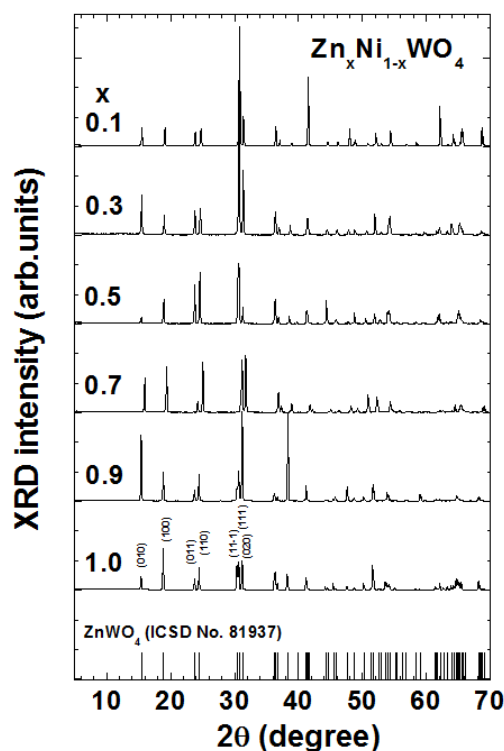


**Figure 1.** X-ray diffraction patterns of the microcrystalline  $ZnWO_4$  and  $Zn_xNi_{1-x}WO_4$  solid solutions annealed at 800°C. (Only a few patterns are shown for clarity).

The photoluminescence spectra were measured using pulsed YAG:Nd laser excitation (4.66 eV, 8 ns) at 20°C. The excitation spectra were collected at room temperature exploiting ultraviolet (UV) and vacuum ultraviolet (VUV) synchrotron radiation (3.6 – 20 eV) emitted from the DORIS III storage ring at the SUPERLUMI station

<sup>1</sup> A. Kuzmin, A. Kalinko, J. Timoshenko, HASYLAB Annual Report 2009:

[http://hasylab.desy.de/annual\\_report/files/2009/2009560.pdf](http://hasylab.desy.de/annual_report/files/2009/2009560.pdf)

(HASYLAB DESY, Hamburg). The measurement procedure has been described in details elsewhere [21, 22].

**Table 1.** Lattice parameters ( $a, b, c, \beta$ ) and unit cell volume ( $V$ ) of monoclinic ( $P2/c$ ) ZnWO<sub>4</sub> ( $x = 1$ ) and Zn<sub>x</sub>Ni<sub>1-x</sub>WO<sub>4</sub> ( $x = 0.1 - 0.9$ ) solid solutions annealed at 800°C.

$x$	$a$ (Å)	$b$ (Å)	$c$ (Å)	$\beta$ (°)	$V$ (Å <sup>3</sup> )
1	4.69	5.72	4.93	90.7	132.4
0.9	4.69	5.73	4.94	90.5	132.9
0.8	4.67	5.69	4.93	90.3	131.1
0.7	4.67	5.70	4.92	90.4	130.9
0.6	4.68	5.70	4.94	90.5	131.5
0.5	4.66	5.70	4.93	90.2	131.1
0.4	4.65	5.70	4.93	90.0	130.7
0.3	4.64	5.69	4.93	90.1	130.3
0.1	4.61	5.68	4.92	90.0	129.0

### 3. Results and discussion

The XRD patterns in Fig. 1 indicate that pure ZnWO<sub>4</sub> and the Zn<sub>x</sub>Ni<sub>1-x</sub>WO<sub>4</sub> solid solutions are formed after annealing at 800°C. The XRD pattern of pure ZnWO<sub>4</sub> was indexed using the standard data (Inorganic Crystal Structure Database (ICSD) No. 81937) for monoclinic ( $P2/c$ ) ZnWO<sub>4</sub> from [20]. Upon substitution of Zn<sup>2+</sup> by Ni<sup>2+</sup> ions, the positions of the Bragg peaks in the XRD patterns shift slightly in the direction of larger scattering angles for increasing nickel content due to a decrease of the lattice parameters (Table 1). Upon increasing nickel content ( $x$ ), the variation of the  $c$  parameter is small ( $\sim 0.01$  Å), but the values of the  $a$  and  $b$  parameters decrease by  $\sim 0.08$  Å and  $\sim 0.04$  Å, respectively. Also the unit cell volume decreases from  $V = 132.4$  Å<sup>3</sup> in ZnWO<sub>4</sub> to  $V = 129.0$  Å<sup>3</sup> in Zn<sub>0.1</sub>Ni<sub>0.9</sub>WO<sub>4</sub>. The results reported in Table 1 are in agreement with that found in the literature for pure tungstates (ZnWO<sub>4</sub> [10, 20] and NiWO<sub>4</sub> [23]) and Zn<sub>x</sub>Ni<sub>1-x</sub>WO<sub>4</sub> solid solutions [10]. Note that the unit cell volume in NiWO<sub>4</sub> ( $V = 127.7$  Å<sup>3</sup>) [23] is expected to be smaller by only about 3.5% than that of ZnWO<sub>4</sub> ( $V = 132.3$  Å<sup>3</sup>) [20].

The phase of the Zn<sub>x</sub>Ni<sub>1-x</sub>WO<sub>4</sub> solid solutions remains monoclinic wolframite-type, and the appearance of any other phases was not observed, in agreement with [10]. Such behaviour can be expected from the close size of Zn<sup>2+</sup> and Ni<sup>2+</sup> ions [24] and is in agreement with previous findings in [10]. Note that the Bragg peaks in the XRD patterns in Fig. 1, for example, the three Bragg peaks (11-1), (111), and (020) located at  $2\theta = 31^\circ$ , are slightly better resolved than in [10].

The photoluminescence spectrum of pure ZnWO<sub>4</sub> powder

consists of a broad band, peaked at about 2.5 eV (Fig. 2). When mixed with NiWO<sub>4</sub>, the Zn<sub>x</sub>Ni<sub>1-x</sub>WO<sub>4</sub> solid solutions are readily formed, and the luminescence spectrum splits into three sub-bands, centred at  $\sim 2.26$  eV,  $\sim 2.5$  eV, and  $\sim 3.0$  eV. Note that the photoluminescence spectra in Fig. 2 have been normalized at the band maximum, and their intensity should not be compared. In fact, addition of nickel results in a reduction of the total photoluminescence signal. We believe that the photoluminescence in the solid solutions has origin similar to that in pure ZnWO<sub>4</sub>, however it is modulated by the self-absorption effect due to the presence of the Ni<sup>2+</sup> ions.

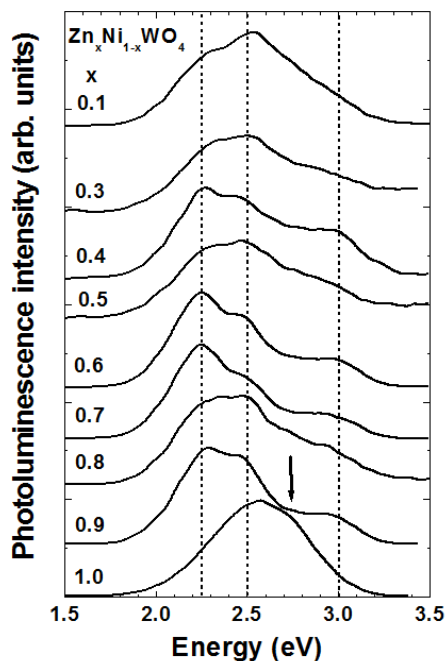


**Figure 2.** Photoluminescence of microcrystalline pure ZnWO<sub>4</sub> ( $x = 1$ ) and the Zn<sub>x</sub>Ni<sub>1-x</sub>WO<sub>4</sub> solid solutions annealed at 800°C.

In pure ZnWO<sub>4</sub> the origin of the main band at 2.5 eV has been previously assigned to radiative electron transitions within the [WO<sub>6</sub>]<sup>6-</sup> anions [11, 12]. At the same time, the band at  $\sim 2.3$  eV has been attributed to recombination of e-h pairs localized at oxygen-atom-deficient tungstate ions [15, 16] or distorted WO<sub>6</sub> octahedra [17].

The origin of the last band at 3.0 eV appearing in the solid solutions is attributed to the interference between the broad luminescence band of the WO<sub>6</sub> groups and the absorption band of the NiO<sub>6</sub> groups. The self-absorption effect is caused by the intensive transition at  $\sim 2.72$  eV from the ground state <sup>3</sup>A<sub>2g</sub> to the excited state <sup>3</sup>T<sub>1</sub> of Ni<sup>2+</sup> (3d<sup>8</sup>) ions [10, 25] in distorted octahedral coordination [23].

The presence of this absorption band results in a notch at 2.7 eV in the emission band, thus making the peak at  $\sim 3.0$  eV more pronounced.

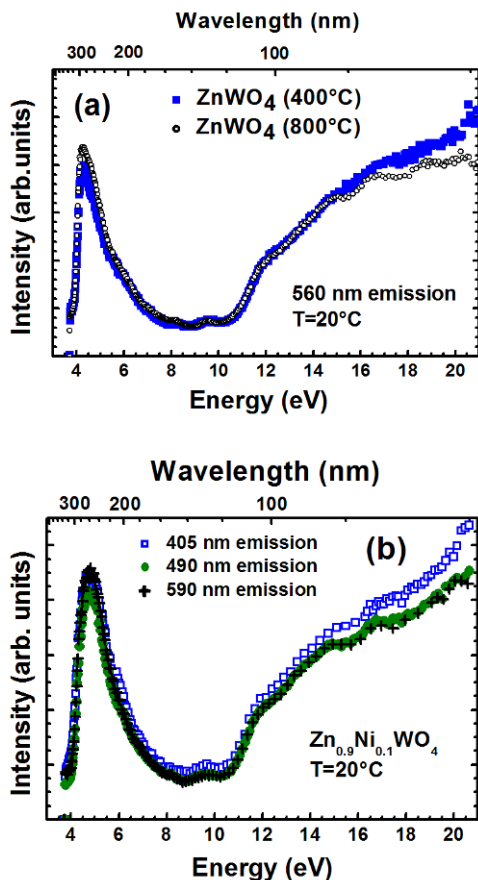


**Figure 3.** Room temperature (20°C) excitation spectra of pure  $\text{ZnWO}_4$  and  $\text{Zn}_{0.9}\text{Ni}_{0.1}\text{WO}_4$ . (a) 560 nm emission in pure  $\text{ZnWO}_4$ , obtained from nano-sized  $\text{ZnWO}_4$  by annealing at 400°C (solid squares) and 800°C (open circles). (b) 405 nm (open squares), 490 nm (solid circles) and 590 nm (crosses) emission in  $\text{Zn}_{0.9}\text{Ni}_{0.1}\text{WO}_4$ .

The excitation spectra are similar for pure  $\text{ZnWO}_4$  and 10% Ni-doped  $\text{ZnWO}_4$  powders (Fig. 3). They consist of a strong band at  $\sim 4.0$  eV having the excitonic origin [11, 12]. The intensity of the excitation spectra starts to grow in the energy region above  $\sim 11$  eV due to the beginning of the multiplication of electronic excitation (MEE) process [11, 12]. In this process, a secondary electron-hole (e-h) pair is created due to the inelastic scattering of a sufficiently 'hot' photoelectron, having an energy exceeding twice that of the band gap value. Further increase of the excitation energy results in deeper valence electrons starting to participate in the MEE process. Finally, when the photon energy reaches  $\sim 17$  eV, i.e.,  $\approx 2E_g + E_V$  where

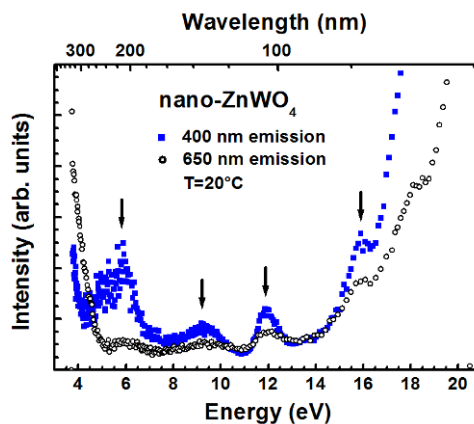


**Figure 4.** Room temperature (20°C) excitation spectra of the 400 nm and 650 nm emissions in pure as-prepared nano-sized  $\text{ZnWO}_4$ , dried in air for 12 hours at 80°C. The bands due to one-electron transitions are indicated by vertical arrows.

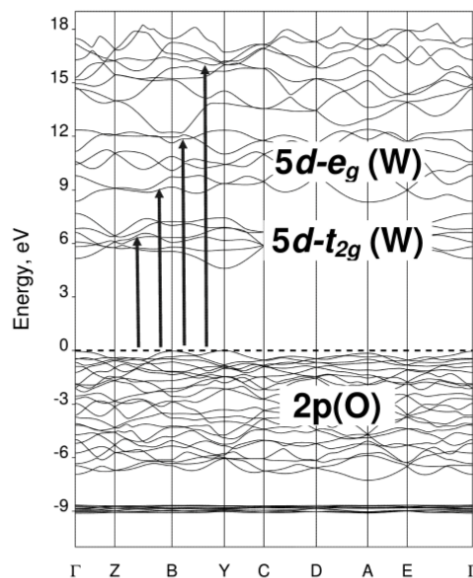


**Figure 5.** Band structure diagram for wolframite-type  $\text{ZnWO}_4$  from [27]. The energy zero is set at the Fermi energy level. The one-electron transitions, corresponding to the peaks (see Fig. 4) in the excitation spectra of nano-sized  $\text{ZnWO}_4$ , are indicated by vertical arrows.

$E_g \approx 4.6 - 4.9$  eV is the band gap energy [11, 26, 27], and  $E_V \approx 7.5$  eV (Fig. 5) is the valence band width [27], the electrons from the bottom of the valence band participate in the MEE process, and the intensity of the excitation spectra exhausts [11, 12]. Note also that the excitation spectra in Fig. 3 are weakly modulated by a fine structure

giving rise to several peaks at about 6, 8, 9.5, 12, 15, and 17 eV: among these the last four peaks are better visible. These energies correlate with the one-electron transitions from the top of the valence band to the conduction band as supported by our LCAO (linear combination of atomic orbitals) calculations [27].

The excitation spectra in nano-ZnWO<sub>4</sub> detected at 400 nm and 650 nm, are close to that from the crystal (Fig. 4). However, a strong band of the excitonic origin is shifted to smaller energies below ~ 4.0 eV, due to a decrease of the optical band gap caused by disorder [28]. The presence of local structural relaxation in nano-ZnWO<sub>4</sub> is confirmed by the extended x-ray absorption fine structure (EXAFS) studies<sup>2</sup> and is in agreement with the recent Raman and luminescence results [19]. A set of peaks observed at 6, 9, 12, and 16 eV in Fig. 4 is attributed to the one-electron transitions from the top of the valence band to quasi-localized states. Such interpretation is in agreement with the first principles LCAO calculations [27] of the band structure for wolframite-type ZnWO<sub>4</sub> (Fig. 5). The LCAO calculations show that the valence band of ZnWO<sub>4</sub>, having largely O 2p character, is separated by the band gap of 4.6 eV from the bottom of conduction band, which is dominated by W 5d states [27]. Therefore, the peaks located between 5 eV and 17 eV in excitation spectra of nano-ZnWO<sub>4</sub> (Fig. 4) are of charge transfer type from oxygen to tungsten.

## 4. Conclusions

The luminescence spectra and luminescence excitation spectra of pure microcrystalline and nano-sized ZnWO<sub>4</sub> and the Zn<sub>x</sub>Ni<sub>1-x</sub>WO<sub>4</sub> solid solutions were studied using vacuum ultraviolet (VUV) synchrotron radiation.

The addition of nickel to ZnWO<sub>4</sub> increases the intensity of emission at ~ 2.3 eV due to a distortion of WO<sub>6</sub> octahedra. The excitation spectra are similar in pure and Zn<sub>0.9</sub>Ni<sub>0.1</sub>WO<sub>4</sub> powders showing strong excitonic band at ~ 4.0 eV and the effect from multiplication of electronic excitation (MEE) process above ~ 11 eV.

The shift of the excitonic band in the excitation spectra of nanosized ZnWO<sub>4</sub> is caused by the local structural relaxation. In nanosized ZnWO<sub>4</sub>, a number of bands is observed in the excitation spectra due to one-electron transitions from the top of the valence band to quasi-localized states.

<sup>2</sup> A. Kuzmin, A. Kalinko, J. Timoshenko, HASYLAB Annual Report 2009: [http://hasylab.desy.de/annual\\_report/files/2009/2009560.pdf](http://hasylab.desy.de/annual_report/files/2009/2009560.pdf)

## Acknowledgements

This work was supported by ESF Project 2009/0202/1DP/1.1.1.2.0/09/APIA/VIAA/141, Latvian Government Research Grant No. 09.1518 and Joint Project No. 10.0032. The research leading to these results has also received funding from the European Community's Seventh Framework Programme (FP7/2007–2013) under grant agreement No. 226716.

## References

- [1] A.W. Sleight, *Acta. Crystallogr. B* 28, 2899 (1972)
- [2] H. Wang, F.D. Medina, D.D. Liu, Y.D. Zhou, *J. Phys.-Condens. Mat.* 6, 5373 (1994)
- [3] H. Kraus et al., *Phys. Lett. B* 610, 37 (2005)
- [4] H. Grassmann, H.G. Moser, E. Lorenz, *J. Lumin.* 33, 21 (1985)
- [5] A.A. Kaminskii, *Appl. Optics* 38, 4533 (1999)
- [6] A.R. Phani, M. Passacantando, L. Lozzi, S. Santucci, *J. Mater. Sci.* 35, 4879 (2000)
- [7] A. Kuzmin, R. Kalendarev, A. Kursitis, J. Purans, *J. Non-Cryst. Solids* 353, 1840 (2007)
- [8] H.M. Pask, *Prog. Quant. Electron.* 27, 3 (2003)
- [9] L.C. Hsu, *Am. Mineral.* 66, 298 (1981)
- [10] A.L.M. de Oliveira et al., *Dyes Pigments* 77, 210 (2008)
- [11] V.N. Kolobanov et al., *Nucl. Instrum. Meth. A* 486, 496 (2002)
- [12] V. Nagirnyi et al., *Nucl. Instrum. Meth. A* 486, 395 (2002)
- [13] V. Pankratov, L. Grigorjeva, D. Millers, S. Chernov, S. Voloshinovskii, *J. Lumin.* 94, 427 (2001)
- [14] L. Grigorjeva, D. Millers, S. Chernov, V. Pankratov, A. Watterich, *Radiat. Meas.* 33, 645 (2001)
- [15] M. Itoh, T. Katagiri, T. Aoki, M. Fujita, *Radiat. Meas.* 42, 545 (2007)
- [16] Z. Lou, J. Hao, M. Cocivera, *J. Lumin.* 99, 349 (2002)
- [17] V.B. Mikhailik, H. Kraus, G. Miller, M.S. Mykhaylyk, D. Wahl, *J. Appl. Phys.* 97, 083523 (2005)
- [18] G. Huang, Y. Zhu, *Mater. Sci. Eng. B-Adv.* 139, 201 (2007)
- [19] A. Kalinko, A. Kuzmin, *J. Lumin.* 129, 1144 (2009)
- [20] P.F. Schofield, K.S. Knight, G. Cressey, *J. Mater. Sci.* 31, 2873 (1996)
- [21] G. Zimmerer, *Radiat. Meas.* 42, 859 (2007)
- [22] V. Pankratov, M. Kirm, H. von Seggern, *J. Lumin.* 113, 143 (2005)
- [23] H. Weitzel, *Z. Kristallogr.* 144, 238 (1976)
- [24] R.D. Shannon, *Acta Crystallogr. A* 32, 751 (1976)
- [25] L.N. Limarenko, A.E. Nosenko, M.V. Pashkovskii,

- D.-L.L. Futorskii, Influence of structural defects on physical properties of tungstates. (Vysha Shkola, Lvov, 1978)
- [26] M. Itoh, N. Fujita, Y. Inabe, J. Phys. Soc. Jpn. 75, 084705 (2006)
- [27] A. Kalinko, A. Kuzmin, R.A. Evarestov, Solid State Commun. 149, 425 (2009)
- [28] E. Orhan et al., J. Solid State Chem. 178, 1284 (2005)